Atmospheric Research 294 (2023) 106988

Contents lists available at ScienceDirect

Atmospheric Research

journal homepage: www.elsevier.com/locate/atmosres

Are thunderstorms linked to the rapid Sea ice loss in the Arctic?

J. Saha [a], C. Price [b], T. Plotnik [c], A. Guha [a,*]

[a] Department of Physics, Tripura University, Agartala, Tripura, India
[b] Porter School of the Environment and Earth Sciences, Department of Geophysics, Tel Aviv University, Israel
[c] Fredy and Nadine Herrmann Institute of Earth Sciences, Hebrew University of Jerusalem, Israel

ARTICLE INFO

Keywords:
Arctic sea ice
Upper tropospheric water vapor (UTWV)
Climate change
Thunderstorms

ABSTRACT

Sea ice in the Arctic grows during the winter and retreats in the summer. The highly reflective white surface of sea ice reflects solar energy, cooling the planet. However, when it melts, the darker ocean absorbs more solar radiation, reinforcing the cycle of melting sea ice. Since sea ice plays a critical role in regulating Earth's climate, changes in sea ice may influence global weather patterns and ocean circulations. In addition to the rise in greenhouse gases in the Arctic, upper tropospheric water vapor (UTWV) or the specific humidity (SH) is also increasing, while acting as an additional greenhouse gas trapping in heat released from the Earth's surface. While annual greenhouse gas concentrations in the Arctic are increasing rather smoothly over time, the interannual variability in sea ice is shown here to be linked to the variability of UTWV at 400 hPa in the Arctic. We propose that increasing thunderstorm activity in the Arctic in the last decade is increasing the water vapor in the upper troposphere, partially explaining the interannual variability, and long term decrease, in the Arctic summer sea ice extent. Both the temporal and spatial analysis between UTWV and Sea Ice changes show that the decline of the summer sea ice cover in the Arctic may be linked to the increasing thunderstorm activity in the Arctic in the last decades.

1. Introduction

The on-going decline of Arctic Sea Ice cover has continued over the time since the start of the satellite records in 1979. While the sea ice returns and grows every winter, the summer extent of Arctic sea ice, and the thickness of the sea ice is decreasing over time. In 2022, Arctic sea ice reached its minimum extent for the year at 4.67 million square kms (1.80 million square miles), according to the NSIDC (https://nsidc.org/arcticseaicenews/). The maximum melting of summer sea ice in the Arctic happens in the months of August, September and October (ASO), delayed from the maximum solar radiation during the summer solstice (June 21). Based on simulations from the latest generation Coupled Model Intercomparison Project Phase 6 (CMIP6) models, a recent study Kim et al., 2023 shows that the first sea ice-free September will occur as early as the 2030s–2050s irrespective of emission scenarios. Extended occurrences of an ice-free Arctic in the early summer months are projected later in the century under higher emissions scenarios. This summertime melting of sea ice impacts the snow-ice-albedo positive feedback (Taylor et al., 2012; Pithan and Mauritsen, 2014), amplifying the near-surface temperatures in the Arctic, with Arctic temperatures rising two to three times faster than the global mean temperatures (Screen and Simmonds, 2010).

This rapid warming of the Arctic has far reaching consequences for the climate of the Earth, and the ecology of the Arctic (Vihma, 2014). While the increasing atmospheric greenhouse gases are driving the average warming of the Arctic, the details of the warming patterns are still uncertain (Gillett et al., 2008). Recent climate models and simulations predicted that during the summer, the Arctic will be ice free by 2050s, while other studies put this time at 2030s (Guarino et al., 2020; Notz et al., 2020). So, are we missing parts of the puzzle?

1.1. Link between UTWV changes and warming surface temperature

The amplification of the Arctic surface temperature is caused by a number of positive feedbacks (Min et al., 2008; Andersson et al., 2021). Normally researchers point to the snow-ice-albedo feedback, as mentioned above. However, one essential positive feedback is related to the rise in upper tropospheric water vapor (UTWV), or specific humidity (SH), that acts as an intense greenhouse gas trapping in additional heat released from the Earth's surface (Hansen et al., 1984). Water vapor is a

* Corresponding author.
E-mail address: anirbanguha@tripurauniv.ac.in (A. Guha).

https://doi.org/10.1016/j.atmosres.2023.106988
Received 11 June 2023; Received in revised form 16 August 2023; Accepted 29 August 2023
Available online 30 August 2023
0169-8095/© 2023 Elsevier B.V. All rights reserved.

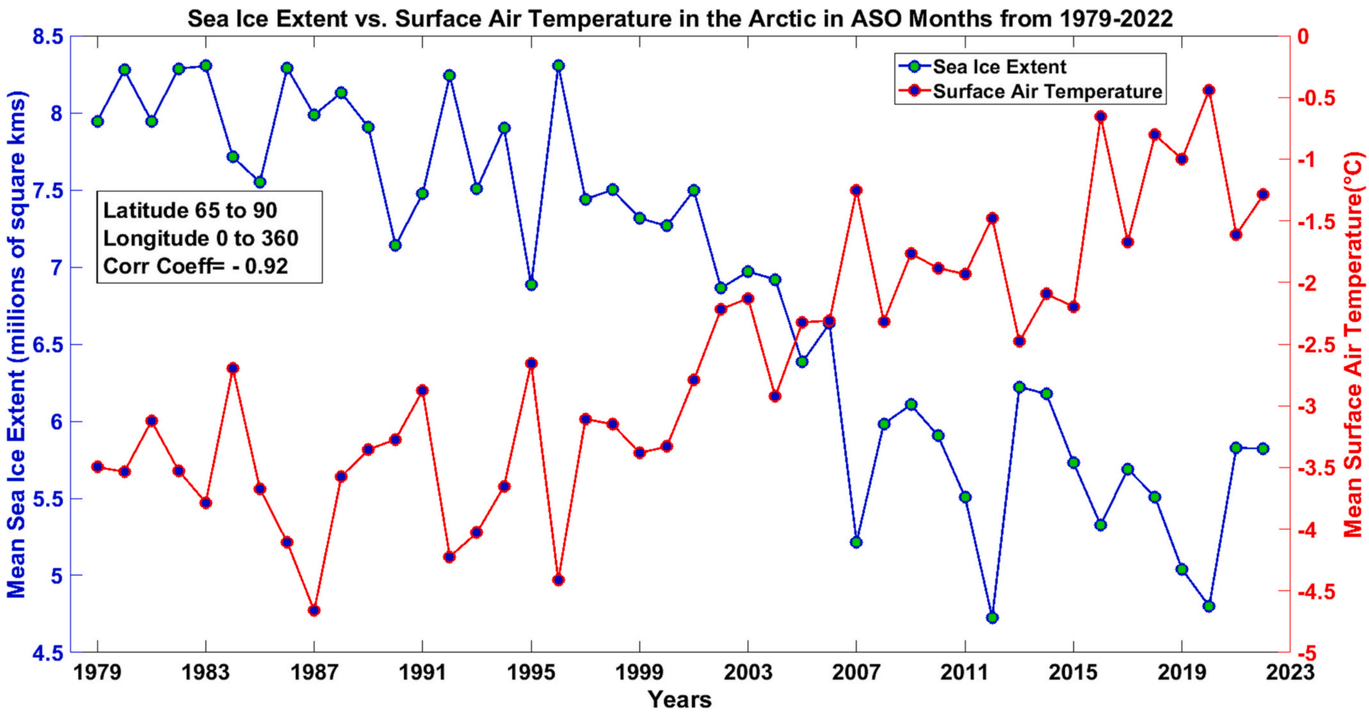

Fig. 1. Time series of the three monthly mean (ASO) for Sea Ice Extent (blue) and three monthly mean (ASO) Surface Air Temperature (red) from 1979 to 2022. (For interpretation of the references to colour in this figure legend, the reader is referred to the web version of this article.)

natural greenhouse gas that traps in infrared radiation emitted by the Earth's surface. In fact, while the Earth's mean surface temperature today is approximately 15 °C, without water vapor in the atmosphere, the globe would have a mean surface temperature of −18 °C! The oceans would be frozen solid. So it is clear from any text book that water vapor acts as a greenhouse gas, warming the Earth's surface temperatures. Furthermore, any increases in water vapor in the atmosphere will amplify the surface warming. Our working hypothesis is that anthropogenic greenhouse gases have resulted in more thunderstorms in the Arctic, that have resulted in more water vapor in the upper troposphere, resulting in more trapping of the longwave radiation from the surface, enhanced surface warming, and causing enhanced sea ice melting in the late summers. It has been shown that tropospheric moistening more than doubles the direct warming effects from carbon dioxide (Dessler et al., 2013) through water vapor feedbacks. Furthermore, increases in upper tropospheric water vapor in response to increasing concentrations of greenhouse gases can result in an additional positive feedback with significant additional surface warming (Del Genio et al., 1994; Colman, 2001). The water-vapor feedback could amplify the surface temperature change due to a doubling of carbon dioxide by up to 60% (IPCC, 1995). Hence, this water vapor feedback is an important component of our climate system (Joshi et al., 2010).

1.2. Link between the thunderstorm and upper tropospheric water vapor

Deep convection in the atmosphere (often including thunderstorms) acts as a huge vacuum cleaner, sucking up boundary layer water vapor and transporting this water vapor through clouds to the upper troposphere. This is the mechanism that brings water vapor to the upper atmosphere. There is new evidence that thunderstorms and deep convection is increasing in the Arctic. The World Wide Lightning Location Network (WWLLN) has shown that lightning strokes above 65°N are increasing linearly with the temperature increases in the Arctic, and lightning activity grew by a factor of 3 as the temperature anomaly increased from 0.65 °C to 0.95 °C (Holzworth et al., 2021). These summer thunderstorms can lead to stronger updrafts and large amounts of water vapor being transported aloft (Sherwood, 1999). There have been numerous studies looking at this link, and there is a well-established link between lightning and upper tropospheric water vapor (UTWV) in other parts of the globe (Price, 2000; Price and Asfur, 2006; Deierling and Petersen, 2008). The intensity of the lightning activity represents the intensity of the convection in these storms, particularly the intensity of the updrafts, and hence the amount of water vapor transported in the upper troposphere (Price and Rind, 1992; Newell et al., 1996). Hence, it has been shown that lightning observations may be a sensitive indicator of the daily variability of UTWV (Price and Asfur, 2006).

The upper tropospheric moisture budget is a balanced between water vapor transported aloft by deep convection, and detrained near the tropopause with compensatory subsidence accompanying the deep convection (Lindzen, 1996). In this paper, we analyse the increasing Arctic summer (JJA) lightning stroke counts above 65°N and the possible implications in the decreasing coverage of late summer Arctic Sea Ice.

2. Database for the present analysis

2.1.1. Specific humidity data

The specific humidity (kg/kg) or the UTWV data at 400 hPa and Surface Air Temperature at 1000 hPa have been obtained from the Copernicus Climate Data Store (https://cds.climate.copernicus.eu) ERA5 Reanalysis Product (Hersbach et al., 2020). This reanalysis datastore provides global climate and weather parameters (mostly atmospheric, ocean-wave, and land-surface quantities) for the last four to five decades. Data have been gridded to a regular lat-long grid of 0.25° for the reanalysis.

2.1.2. Sea ice extent data

We have obtained the Sea Ice extent (in millions of square kms) data

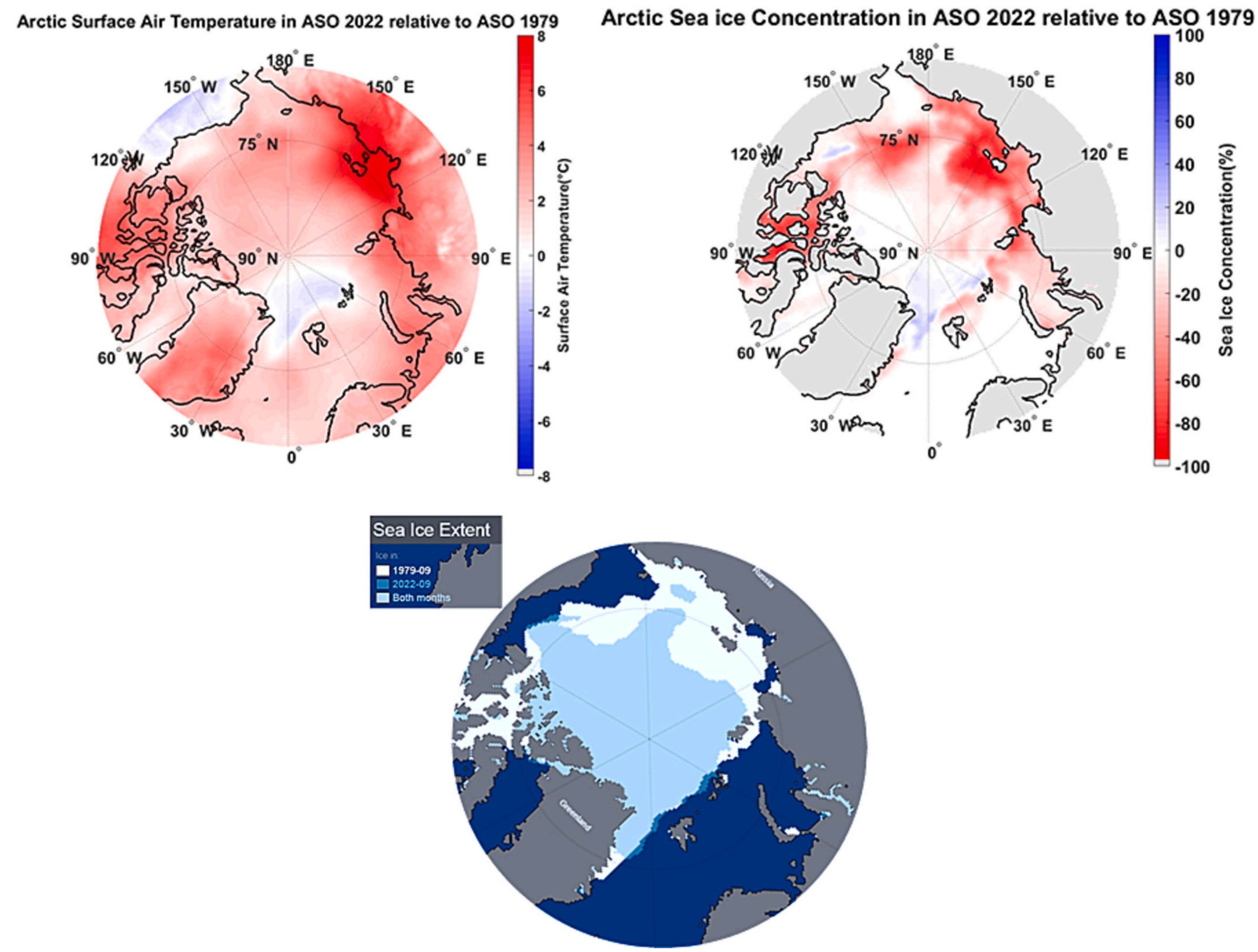

Fig. 2. Spatial comparison of the changes in ASO Surface Air Temperature (°C) and ASO Sea Ice Concentration between 2022 and 1979 in the Arctic north of 65°N. The Sea Ice Extent plot gives the visual distribution of the ASO ice coverage in September 2022 (blue) and September 1979 (white). (For interpretation of the references to colour in this figure legend, the reader is referred to the web version of this article.)

from NSIDC which provides the changes in Sea Ice in the Arctic and the Antarctic (Fetterer et al., 2017). NSIDC provides the data from the satellites DMSP F-16, DMSP, F-17, and DMSP F-18 from the Defence Meteorological Satellite Program (DMSP) series of satellites, and from the Nimbus-7 (https://nsidc.org/data/g02135/versions/3). Spatial resolution of the data is 25 km.

2.1.3. *Sea ice concentration data*

In addition, Sea Ice concentration (in percentage) data are derived from the European Organisation for the Exploitation of Meteorological Satellites (EUMETSAT) Ocean and Sea Ice Satellite Application Facility (OSI SAF). This product is based on the sensors Scanning Multichannel Microwave Radiometer (SMMR; 1979–1987), Special Sensor Microwave/Imager (SSM/I; 1987–2006), and Special Sensor Microwave Imager/Sounder (SSMIS; 2005 onward). This is the phase 1 data and referred to as the SSMIS product. SSMIS product is giving data for last 40-year having a grid resolution of 25 km (https://osi-saf.eumetsat.int/products/osi-401-b) (Andersen et al., 2007).

2.1.4. *Lightning data*

The thunderstorm data are derived from the lightning stroke count observed by the World Wide Lightning Location Network (WWLLN) (Link: https://wwlln.net/) made up of around 70 very low frequency (VLF), 3–30 kHz sensors distributed around the globe (Virts et al., 2013; Kaplan and Lau, 2022). The WWLLN detects VLF electromagnetic waves generated by individual lightning strokes. The WWLLN detection efficiency is highly dependent on the non-uniform distribution of WWLLN sensors around the world. To minimize the detection efficiency changes over time, we normalised the stroke count data in the Arctic by dividing the total number of detected strokes above 65°N by the total number of global WWLLN-observed strokes in that summer season (JJA) (Holzworth et al., 2021). Hence, our lightning statistics show the percentage of the total global lightning in the Arctic. It is estimated that the WWLLN system detects 30% of all cloud-to-ground lightning flashes.

3. Observational results

We know that late summer Arctic sea ice has been decreasing in area since the start of daily monitoring by satellites in 1979. Arctic sea ice shows its minimum extension during the months of August, September and October (ASO), after the warm summer, every year (https://nsidc.org/arcticseaicenews/charctic-interactive-sea-ice-graph/).

Fig. 1 shows the link between the changes in Sea Ice Area (ASO) with the Surface Air Temperatures in the Arctic (ASO). The upward trend of Surface Air Temperature and the decreasing trend of Sea Ice in the Arctic shows a strong anti-correlation ($r = -0.92$) and the result is statistically

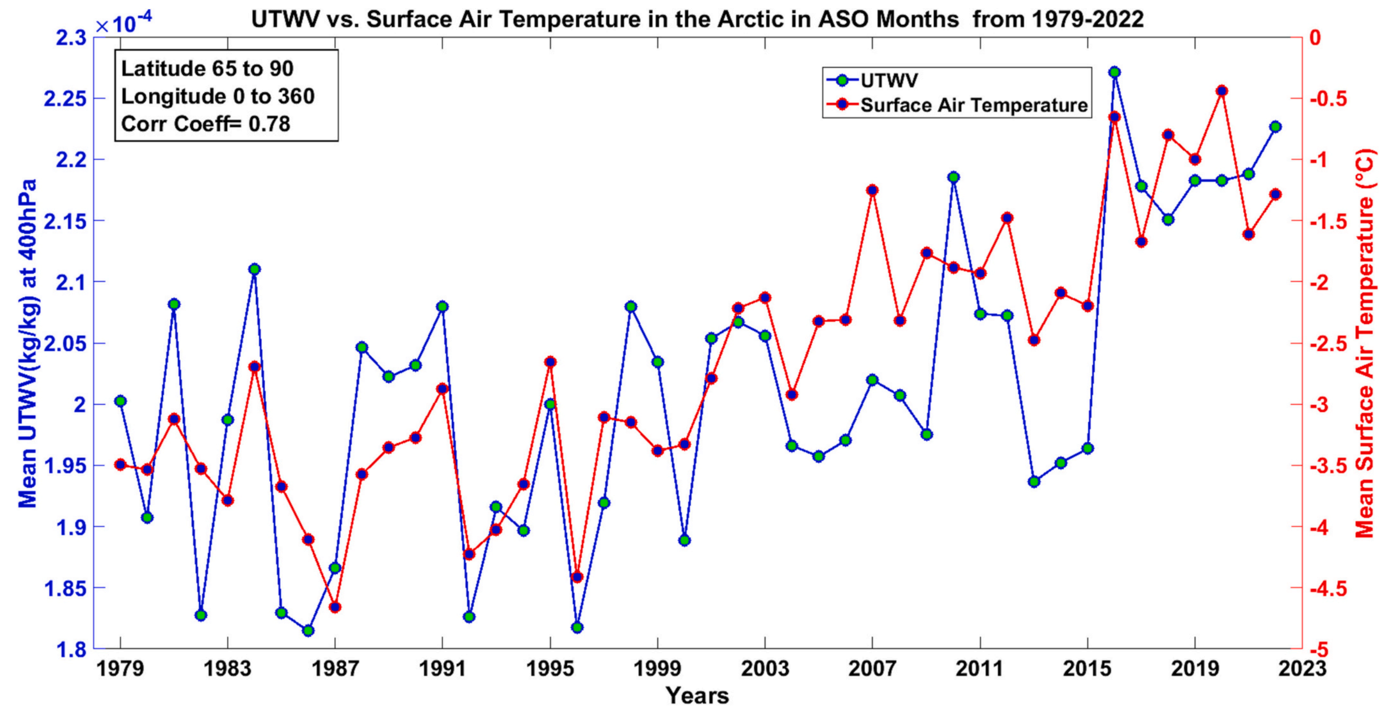

Fig. 3. Time series of ASO UTWV (blue) and ASO Surface Air Temperature (red) from 1979 to 2022. ASO is used since this is when we observe the minimum sea ice coverage in the Arctic. (For interpretation of the references to colour in this figure legend, the reader is referred to the web version of this article.)

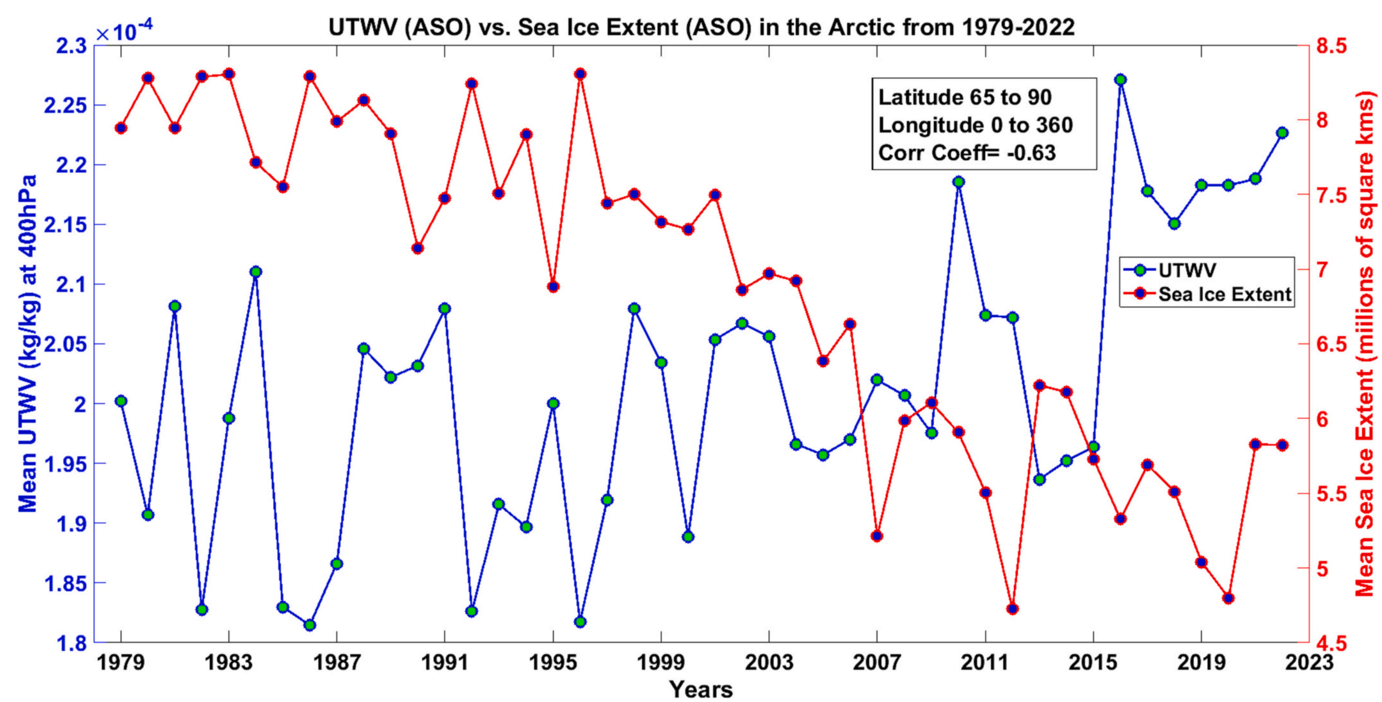

Fig. 4. Time series of ASO UTWV (blue) and ASO Sea Ice Extent (red) from 1979 to 2022. (For interpretation of the references to colour in this figure legend, the reader is referred to the web version of this article.)

significant at 95% significance level. We point out that the detrended curves are also highly correlated with a correlation coefficient of $r = -0.71$.

Fig. 2 shows that the spatial change (from 1979 to 2022) in the anomalies of Surface Air Temperature (°C) and Sea Ice Concentration (%) in the months of ASO. Note that the colour bar was flipped between the left and right panels. Higher Surface Air Temperatures (red) are related to less sea ice coverage (red). The locations with the highest Surface Air Temperature increases are the same areas where the sea ice concentrations have decreased the most over the last 40 years. Especially, between 70°E to 170°E (Arctic coast of Northern Russia) and 90°W to 120°W (Northern Canada). We also show the ice coverage (Sea Ice Extent map from NSIDC; Link: https://nsidc.org/arcticseaicenews/sea-ice-comparison-tool/) in September 2022 (blue) compared with the

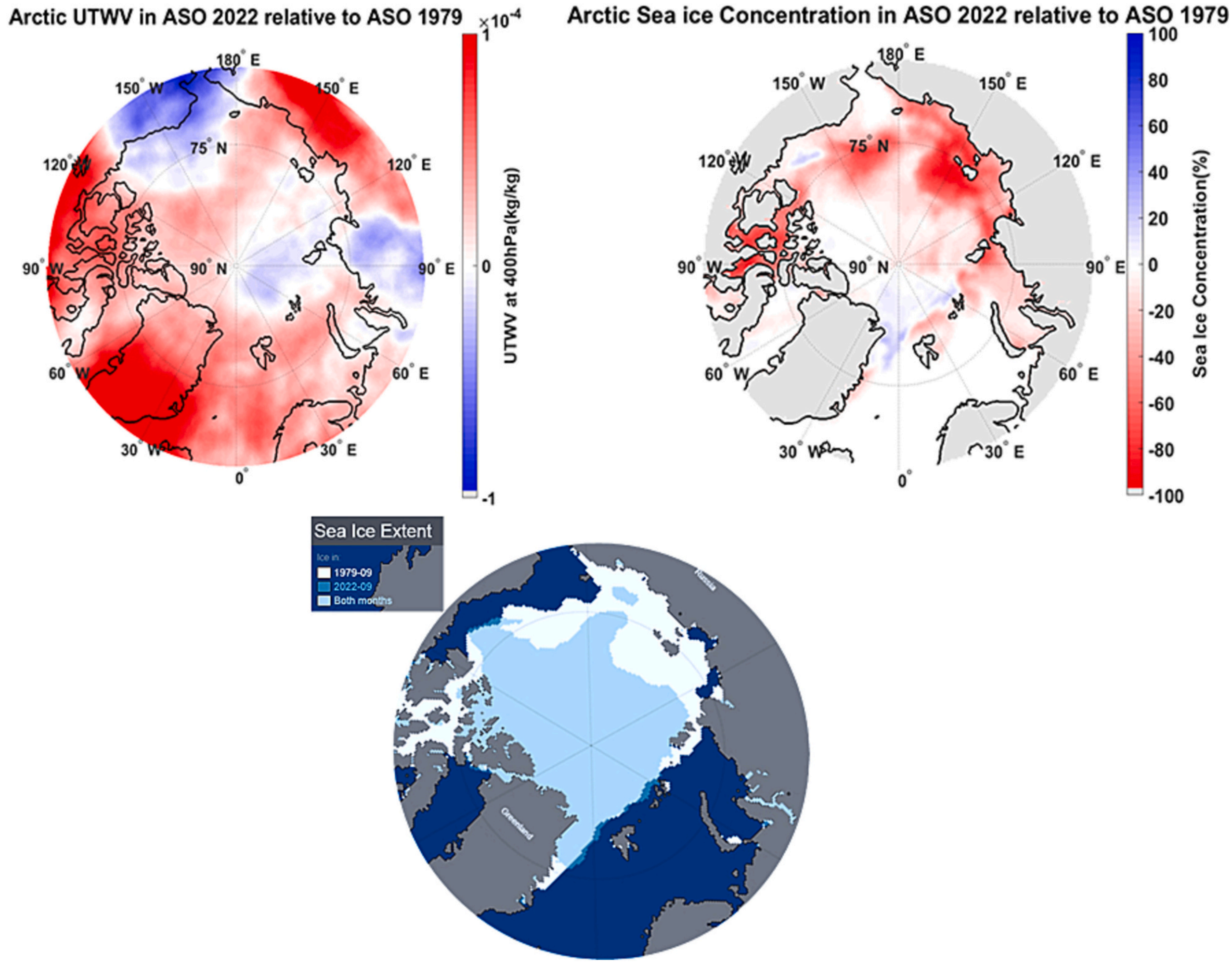

Fig. 5. Spatial comparison of ASO UTWV and ASO Sea Ice Concentration in 2022 relative to 1979 in the Arctic. The Sea Ice Extent plot gives the visual idea of how the ice coverage in September 2022 (indigo) was reduced compared with September 1979 (white). (For interpretation of the references to colour in this figure legend, the reader is referred to the web version of this article.)

ice coverage in September 1979 (white). The regions is white are the areas where sea ice has disappeared since 1979, and is where we see the maximum warming.

What causes the interannual variability of the temperature and sea ice values? The rise in greenhouse gases over the Arctic has been quite smooth over the years, with little interannual variability. We suggest that this is due to changes in the upper tropospheric water vapor (UTWV) in the Arctic. We propose that this UTWV is related to the changes in storm activity in the Arctic over the past decade, and in particular the increase in convective storms in the summer months. As water vapor is a natural greenhouse gas, increases in water vapor in the upper atmosphere will amplify the initial warming due to increasing anthropogenic greenhouse gases, resulting in a positive feedback. Fig. 3 shows that the UTWV (ASO months) and Surface Air Temperature (ASO months) are rising hand-in-hand for over 44 years from 1979 to 2022. The correlation coefficient between these two time-series is 0.78. Here the *p*-value is 6.348e-10. If we look at the detrended time series, the correlation coefficient is 0.66, still highly significant statistically.

Finally, Fig. 4 shows that the negative correlation ($r = -0.63$) between the UTWV at 400 hPa and the Sea Ice Extent for the period of 1979 to 2022. We have analysed the UTWV at other pressure levels, but the best correlations with sea ice are for 400 hPa. As can often be seen, years with high levels of UTWV are associated with years with minimum sea ice coverage in ASO. Here the p-value is 0.000003924. Here too, the detrended data show a correlation coefficient of −0.33 which is still statistically significant at the 95% level.

Fig. 5 shows that the change in spatial distribution of UTWV (kg/kg) at 400 hPa and Sea Ice Coverage (%) in the months of ASO in 2022 relative to the same months of 1979. The colour bar is flipped between the left and right panels. More UTWV (red) is related to less sea ice coverage (red), similar to Fig. 2. Increasing UTWV results in a decrease of sea ice coverage in the region 100°E to 170°E (Northern Russia) and 80°W to 130°W (Northern Canada). Here also, we present the visualization of how the ice coverage (Sea Ice Extent map from NSIDC; Link: https://nsidc.org/arcticseaicenews/sea-ice-comparison-tool/) has changes between September 1979 (white) and September 2022/09 (blue).

The total lightning strokes above 65°N, normalised by the total global strokes, for the period 2011 to 2021 observed by the WWLLN is shown in Fig. 6. Unfortunately, we only have 12 years of stable reliable data from the WWLNN network, and hence cannot extend our timeseries back to 1979. We minimize the possible influence of the changing WWLLN network detection efficiency by normalizing strokes above 65°N by the total global strokes (Holzworth et al., 2021). As shown, the Arctic lightning activity dominates during the Northern Hemisphere summer each year (JJA). However, beyond the main summertime period in JJA months, there are lightning strokes in the months of May and September. Therefore, we consider May, June, July, August and September (MJJAS) in our lightning analysis. The trend shows that above 65°N there is an increase with time, indicating that the Arctic is

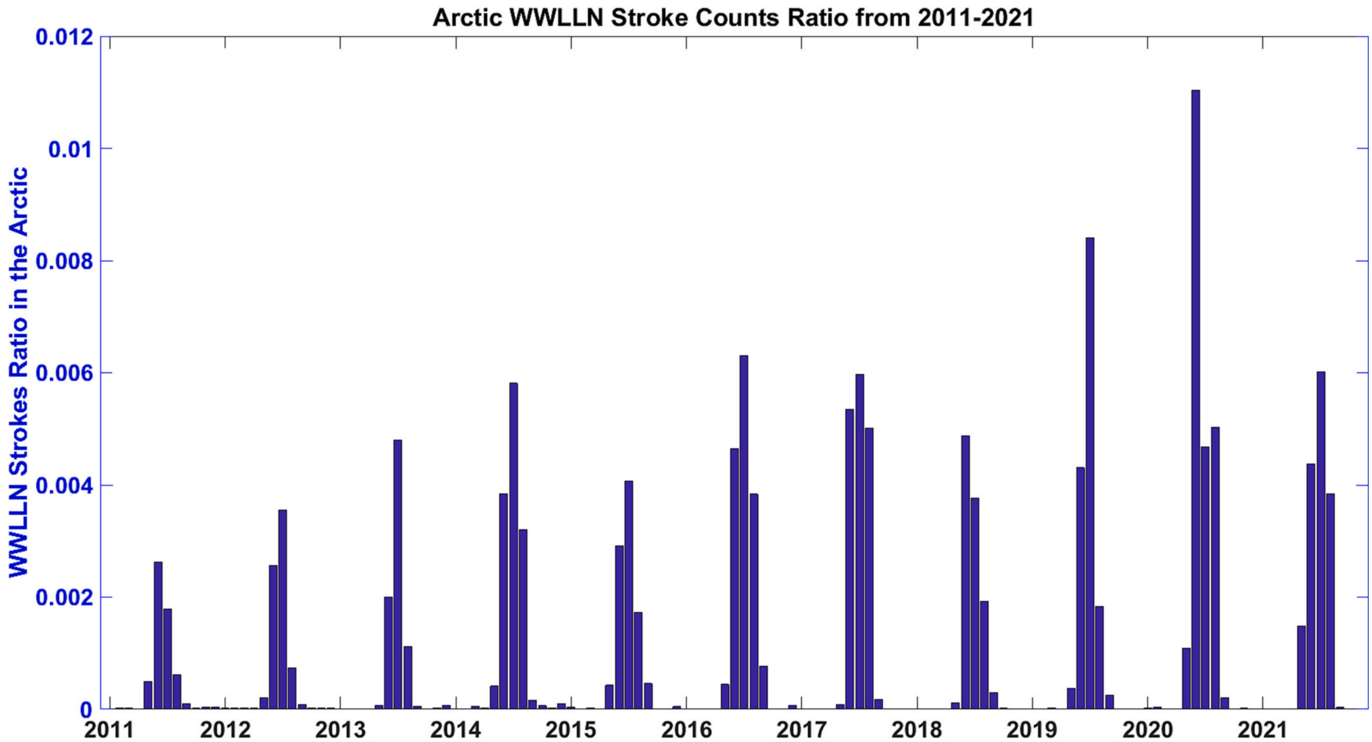

Fig. 6. Lightning strokes above 65°N normalised by the total global strokes for the period 2011 to 2021 observed by the WWLLN.

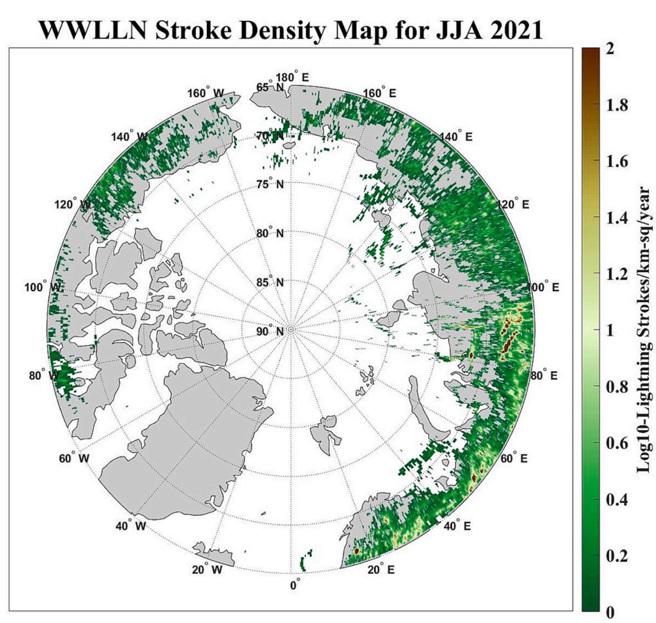

Fig. 7. Spatial distribution of lightning stroke density (strokes/ km^2/year) in June, July and August (JJA) months of 2021 above 65°N.

becoming more influenced by thunderstorms and convective storms in the summer months. We note that 2020 had the largest amount of lightning in the Arctic in the last decade, and was also a year with very lowest Sea Ice coverage at the end of the summer of 2020.

Fig. 7 shows the spatial lightning stroke density (*strokes/ km^2/year)* detected by the WWLLN lightning network. It is produced by combining the data for the period of June, July and August 2021 into a single set of observations and binning them into lat-lon bins (1°x1°). Lightning density in the Arctic is quite low and such a colour scale was chosen to accentuate the observations. We see that the distribution of Arctic lightning stroke density pole-ward of 65°N latitude is dominated by lightning at longitudes of 20°E to 170°E (Scandinavia and Northern Russia) and 120°W to 160°W (Northern Canada and Alaska).

Note that at these latitudes in the summer the mean wind flow is westerly in direction, resulting in the transport of UTWV eastwards from the source regions.

Fig. 8 shows the time series correlation plot of normalised WWLLN lightning strokes (total lightning strokes above 65°N divided by global lightning strokes) in the Arctic summer (MJJAS months) vs. UTWV in the ASO months ($r = 0.69$, $p = 0.03787$) from 2013 to 2021. For UTWV, each data point is a mean for the Specific Humidity (UTWV) for the three months (ASO) average at 400 hPa between 65°N-90°N (Arctic). The trend of the time series in this figure strongly reflects the consistent increasing trend of UTWV along with the increasing lightning stroke counts.

Fig. 9 shows the time series correlation plot of Sea Ice Extent in the ASO months vs. normalised WWLLN lightning strokes (total lightning strokes above 65°N divided by global lightning strokes) in the Arctic summer (MJJAS months) ($r = -0.70$) over the last decade (2013 to 2021). Here, *p*-value is 0.04149. While we are limited with the amount of Arctic lightning data, it is clear that the year with the most lightning (2020) had the largest melting of sea ice, while the year with the least lightning (2013) was the year with the most sea ice coverage.

4. Discussion and conclusions

The accelerating decline of Arctic Sea Ice over the past decades is related to the increasing temperatures of the Arctic over the same period. Furthermore, the primary reason behind the rising temperatures is the increasing emission of anthropogenic greenhouse gases (Notz and Stroeve, 2016; Ding et al., 2017; Stroeve and Notz, 2018). Both climate models and observations support the idea of a positive water vapor feedback; that is, higher surface temperatures will increase the amount of deep convection, that will lead to more UTWV, further enhancing the surface warming (Rind et al., 1991; Rind, 1998; Del Genio et al., 1994). Decadal variations show substantial changes in the UTWV (Sun and

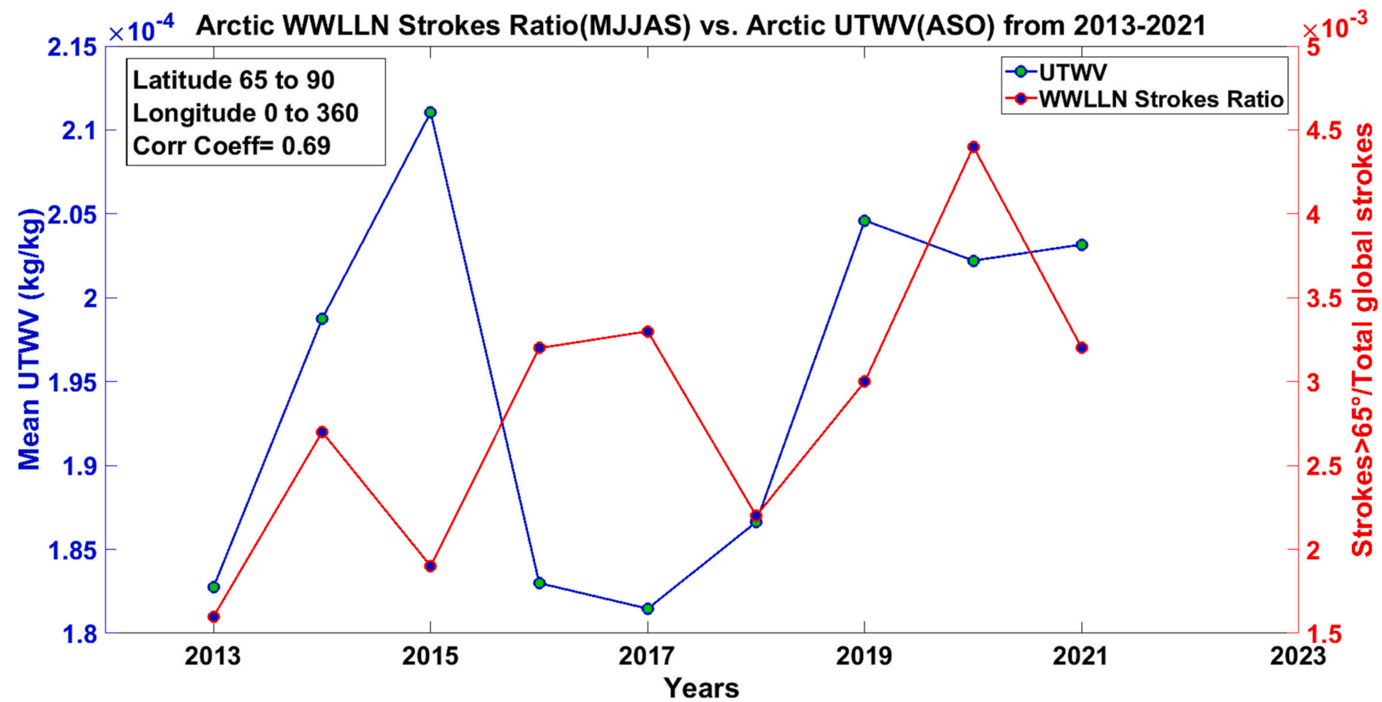

Fig. 8. Time series of UTWV (blue) in ASO months and the normalised WWLLN lightning strokes (red) in MJJAS months from 2013 to 2021. (For interpretation of the references to colour in this figure legend, the reader is referred to the web version of this article.)

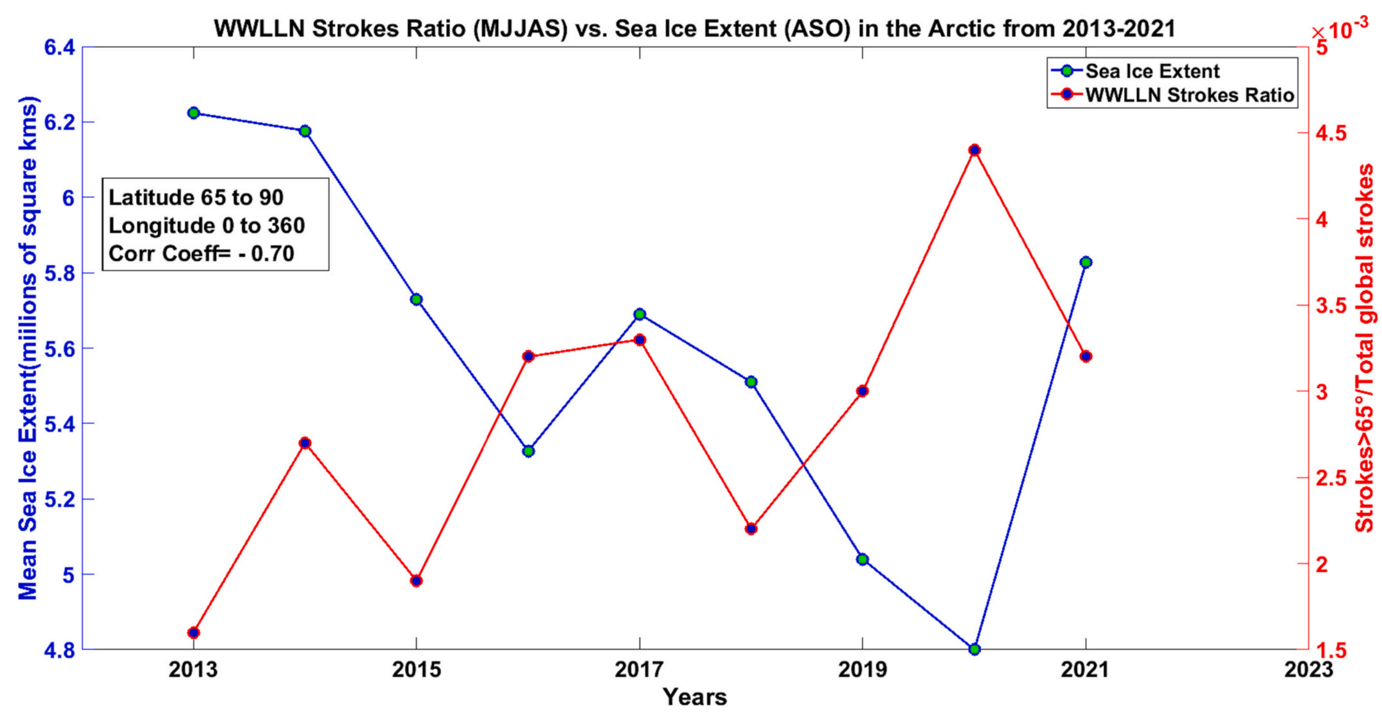

Fig. 9. Time series of normalised WWLLN lightning strokes (red) in MJJAS months and Sea Ice Extent (blue) in ASO months from 2013 to 2021. (For interpretation of the references to colour in this figure legend, the reader is referred to the web version of this article.)

Held, 1996; Chung et al., 2014). Hence, long-term monitoring of UTWV changes, and understanding causes responsible for such changes are necessary for our confidence in the prediction of future climate change (Tian et al., 2013; Chung et al., 2014). We already know that there is a substantial correspondence between accelerating loss of sea ice during ASO and the increasing surface air temperatures in those months ($r = -0.92$). However, our study suggests that the increases in temperatures, and particularly the interannual variability, are primarily due to increases in UTWV that act as an additional major greenhouse agent contributing to the surface warming of the Arctic. We suggest that a significant fraction of the water vapor is transported to the upper troposphere via summer thunderstorms, first as liquid droplets and ice particles in deep convective clouds, and later evaporating/sublimating in the upper troposphere (Kent et al., 1995). In fact, our study shows that there is a strong correlation between Surface Air Temperature and UTWV over the last 40 years ($r = 0.78$) during the months of maximum sea ice melt (ASO). As a consequence, the negative correlation ($r = -0.63$) between the UTWV and the Sea Ice Extent implies UTWV explains nearly 40% of the variability in the coverage of Sea Ice during the period of minimum annual ice extent. In addition to the temporal agreement, we also present the spatial agreement between increasing UTWV and decreases of sea ice coverage (see Fig. 5) in the Arctic between 100°E to 170°E (Northern Russia) and 80°W to 130°W (Northern Canada). Since previous studies have shown that UTWV is closely linked to thunderstorm activity (Price, 2000, Price and Asfur, 2006), we conclude from both the temporal and spatial analysis between UTWV changes and ice cover changes that increasing thunderstorm activity in the Arctic in the last decade (Romps et al., 2014; Holzworth et al., 2021) has contributed to the interannual and long term ice loss at the end of the summer.

Regarding the causality of the statistical relationship presented in our paper. We have looked at the link between lightning in the summer months (MJJAS) and the minimum sea ice every year that occurs in ASO. Hence, the lightning in the summer months are statistically connected to the sea ice coverage at the end of the summer (ASO). While the lightning in the Arctic is related to convective storms, atmospheric instabilities and solar heating (with a peak in JJA), the sea ice does not respond immediately to the solar forcing. There is always a lag between solar radiation and ocean temperatures, atmospheric warming, and water vapor concentrations in the atmosphere. The consistent increasing trend of UTWV along with the increasing lightning stroke counts in the Arctic supports the fact that thunderstorms that occur in the summer months (especially MJJAS) leave high concentrations of UTWV in the upper troposphere for months after the storms, impacting the surface heating of the Arctic, and the minimum sea ice content even in ASO. Hence, although correlation does not imply causation, it is clear that increased summer convection (and lightning) will impact the sea ice extent a few months later, and not the reverse. For the reverse relationship to be valid, we would have to be able to explain how the sea ice decrease in ASO impacts the thunderstorms a few months earlier. This is highly unlikely to be the case. Hence, northern hemisphere summertime (MJJAS) increasing lightning appears to be a defining factor in the temporal and spatial changes in sea ice coverage in the Arctic summer.

CRediT authorship contribution statement

J. Saha: Conceptualization, Formal analysis, Methodology, Data curation, Software, Visualization, Writing – original draft. **C. Price:** Supervision, Conceptualization, Methodology, Investigation, Visualization, Funding acquisition, Project administration, Validation, Writing – review & editing. **T. Plotnik:** Methodology, Visualization, Data curation. **A. Guha:** Supervision, Conceptualization, Investigation, Visualization, Funding acquisition, Project administration, Resources, Software, Validation.

Declaration of Competing Interest

The authors whose names are listed immediately below certify that they have NO affiliations with or involvement in any organisation or entity with any financial interest (such as honoraria; educational grants; participation in speakers' bureaus; membership, employment, consultancies, stock ownership, or other equity interest; and expert testimony or patent-licensing arrangements), or non-financial interest (such as personal or professional relationships, affiliations, knowledge or beliefs) in the subject matter or materials discussed in this manuscript.

Data availability

No new data were used in this paper.

Acknowledgements

This work acknowledges using the valuable Specific Humidity data and the Air Temperature data from ERA5 reanalysis product of Copernicus Climate Data store (https://cds.climate.copernicus.eu). The National Snow and Ice Data Center (NSIDC) provided the changes in Sea Ice Extent data (https://nsidc.org/data/g02135/versions/3). This work also acknowledges European Organisation for the Exploitation of Meteorological Satellites (EUMETSAT) for providing the Sea Ice Concentration data (https://osi-saf.eumetsat.int/products/osi-401-b). The authors wish to thank the members of World Wide Lightning Location Network (WWLLN) for contributing their data to (https://wwlln.net/).

The authors are also thankful to the University Grant Commission (UGC) of India and the Israel Science Foundation (ISF) for funding the project with UGC funds reference No. F.6-112018(IC). In addition, an acknowledgment is due to the Department of Science and Technology for a supporting fund to the Department of Physics, Tripura University through DST-FIST fund reference SR/FST/PSI-191/2014.

References

Andersen, Søren, Tonboe, Rasmus, Kaleschke, Lars, Heygster, Georg, Pedersen, Leif Toudal, 2007. Intercomparison of passive microwave sea ice concentration retrievals over the high-concentration Arctic Sea ice. J. Geophys. Res. 112 (C8), C08004. https://doi.org/10.1029/2006jc003543.

Andersson, T.R., Hosking, J.S., Pérez-Ortiz, M., et al., 2021. Seasonal Arctic Sea ice forecasting with probabilistic deep learning. Nat. Commun. 12, 5124. https://doi.org/10.1038/s41467-021-25257-4.

Chung, E.-S., Soden, B., Sohn, B.J., Shi, L., 2014. Upper-tropospheric moistening in response to anthropogenic warming. Proc. Natl. Acad. Sci. 111 (32), 11636–11641. https://doi.org/10.1073/pnas.1409659111.

Colman, R., 2001. On the vertical extent of atmospheric feedbacks. Clim. Dyn. 17, 391–405. https://doi.org/10.1007/s003820000111.

Deierling, W., Petersen, W.A., 2008. Total lightning activity as an indicator of updraft characteristics. J. Geophys. Res. 113 (D16) https://doi.org/10.1029/2007jd009598.

Del Genio, A.D., Kovari Jr., W., Yao, M.-S., 1994. Climatic implications of the seasonal variation of upper troposphere water vapor. Geophys. Res. Lett. 21, 2701–2704. https://doi.org/10.1029/94GL02658.

Dessler, A.E., Schoeberl, M.R., Wang, T., Davis, S.M., Rosenlof, K.H., 2013. Stratospheric water vapor feedback. Proc. Natl. Acad. Sci. 110 (45), 18087–18091. https://doi.org/10.1073/pnas.1310344110.

Ding, Q., Schweiger, A., L'Heureux, M., Battisti, D.S., Po-Chedley, S., Johnson, N.C., Steig, E.J., 2017. Influence of high-latitude atmospheric circulation changes on summertime Arctic Sea ice. Nat. Clim. Chang. 7 (4), 289–295. https://doi.org/10.1038/nclimate3241.

Fetterer, F., Knowles, K., Meier, W.N., Savoie, M., Windnagel, A.K., 2017. Sea Ice Index, Version 3 [Data Set]. National Snow and Ice Data Center, Boulder, Colorado USA. https://doi.org/10.7265/N5K072F8.

Gillett, N.P., Stone, D.A., Stott, P.A., Nozawa, T., Karpechko, A.Y., Hegerl, G.C., Jones, P.D., 2008. Attribution of polar warming to human influence. Nat. Geosci. 1 (11), 750–754. https://doi.org/10.1038/ngeo338.

Hansen, J., Lacis, A., Rind, D., Russell, G., Stone, P., Fung, I., Lerner, J., 1984. Climate sensitivity: analysis of feedback mechanisms. Geophys. Monogr. Ser. 130–163 https://doi.org/10.1029/gm029p0130.

Hersbach, H., Bell, B., Berrisford, P., Hirahara, S., Horányi, A., Muñoz-Sabater, J., Thépaut, J., 2020. The ERA5 global reanalysis. Q. J. R. Meteorol. Soc. https://doi.org/10.1002/qj.3803.

Holzworth, R.H., Brundell, J.B., McCarthy, M.P., Jacobson, A.R., Rodger, C.J., Anderson, T.S., 2021. Lightning in the Arctic. Geophys. Res. Lett. 48, e2020GL091366 https://doi.org/10.1029/2020GL091366.

IPCC, 1995. Climate Change Assessment Report; Houghton, J.J., Ed, 1996. Cambridge University Press, Cambridge, UK.

Joshi, M.M., Webb, M.J., Maycock, A.C., Collins, M., 2010. Stratospheric water vapour and high climate sensitivity in a version of the HadSM3 climate model. Atmos. Chem. Phys. 10 (15), 7161–7167. https://doi.org/10.5194/acp-10-7161-2010.

Kaplan, J.O., Lau, K.H.-K., 2022. World wide lightning location network (WWLLN) global lightning climatology (WGLC) and time series, 2022 update. Earth Syst. Sci. Data 14, 5665–5670. https://doi.org/10.5194/essd-14-5665-2022.

Kent, G.S., Williams, E.R., Wang, P.-H., McCormick, M.P., Skeens, K.M., 1995. Surface Temperature Related Variations in Tropical Cirrus Cloud as measured by SAGE II. J. Clim. 8 (11), 2577–2594. https://doi.org/10.1175/1520-0442(1995)008<2577:strvit>2.0.co;2.

Kim, Y.H., Min, S.K., Gillett, N.P., et al., 2023. Observationally-constrained projections of an ice-free Arctic even under a low emission scenario. Nat. Commun. 14, 3139. https://doi.org/10.1038/s41467-023-38511-8.

Lindzen, R.S., 1996. The importance and nature of the water vapor budget in nature and models. In: Treut, H.L. (Ed.), Climate Sensitivity to Radiative Perturbations. NATO ASI Series, vol. 34. Springer, Berlin, Heidelberg. https://doi.org/10.1007/978-3-642-61053-0_5.

Min, S.-K., Zhang, X., Zwiers, F.W., Agnew, T., 2008. Human influence on Arctic Sea ice detectable from early 1990s onwards. Geophys. Res. Lett. 35 https://doi.org/10.1029/2008GL035725.

Newell, R.E., Zhu, Y., Browell, E.V., Read, W.G., Waters, J.W., 1996. Walker circulation and tropical upper tropospheric water vapor. J. Geophys. Res.-Atmos. 101 (D1), 1961–1974. https://doi.org/10.1029/95jd02275.

Notz, D., Stroeve, J., 2016. Observed Arctic Sea-ice loss directly follows anthropogenic CO 2 emission. Science 354 (6313), 747–750. https://doi.org/10.1126/science.aag2345.

Notz, Dirk, Dorr, Jakob, Bailey, David A., Blockley, E.D., Bushuk, Mitchell, Debernard, Jens Boldingh, Dekker, Evelien, De Repentigny, Patricia, Docquier, David, Fukar, Neven S., Fyfe, John C., Jahn, Alexandra, Holland, Marika, Hunke, Elizabeth, Iovino, Doroteaciro, Khosravi, Narges, Massonnet, Franois, Madec, Gurvan, O'Farrell, Siobhan, Petty, Alek, Rana, Arun, Roach, Lettie, Rosenblum, Erica, Rousset, Clement, Semmler, Tido, Stroeve, Julienne, Tremblay, Bruno, Toyoda, Takahiro, Tsujino, Hiroyuki, Vancoppenolle, Martin, 2020. Arctic Sea ice in CMIP6. Geophys. Res. Lett. https://doi.org/10.1029/2019GL086749.

Pithan, F., Mauritsen, T., 2014. Arctic amplification dominated by temperature feedbacks in contemporary climate models. Nat. Geosci. 7 (3), 181–184. https://doi.org/10.1038/ngeo2071.

Price, C., 2000 Jul 20. Evidence for a link between global lightning activity and upper tropospheric water vapour. Nature. 406 (6793), 290–293. https://doi.org/10.1038/35018543 (PMID: 10917527).

Price, C., Asfur, M., 2006. Can lightning observations be used as an indicator of upper-tropospheric water vapor variability? Bull. Am. Meteorol. Soc. 87 (3), 291–298. https://doi.org/10.1175/bams-87-3-291.

Price, Colin, Rind, David, 1992. A simple lightning parameterization for calculating global lightning distributions. J. Geophys. Res.-Atmos. 97 (D9), 9919–9933. https://doi.org/10.1029/92jd00719.

Rind, D., 1998. Justadd water vapor. Science 281, 1152–1153.

Rind, D., Chiou, E.W., Chu, W., et al., 1991. Positive water vapour feedback in climate models confirmed by satellite data. Nature 349, 500–503. https://doi.org/10.1038/349500a0.

Romps, D.M., Seeley, J.T., Vollaro, D., Molinari, J., 2014. Projected increase in lightning strikes in the United States due to global warming. Science 346 (6211), 851–854. https://doi.org/10.1126/science.1259100.

Screen, J.A., Simmonds, I., 2010. The central role of diminishing sea ice in recent Arctic temperature amplification. Nature 464 (7293), 1334–1337. https://doi.org/10.1038/nature09051.

Sherwood, Steven C., 1999. On moistening of the tropical troposphere by cirrus clouds. J. Geophys. Res. 104 (D10), 11949. https://doi.org/10.1029/1999jd900162.

Guarino, Maria-Vittoria, Sime, Louise C., Schröeder, David, Malmierca-Vallet, Irene, Rosenblum, Erica, Ringer, Mark, Ridley, Jeff, Feltham, Danny, Bitz, Cecilia, Steig, Eric J., Wolff, Eric, Stroeve, Julienne, Sellar, Alistair, 2020. Sea-ice-free Arctic during the last interglacial supports fast future loss. Nat. Clim. Chang. https://doi.org/10.1038/s41558-020-0865-2.

Stroeve, J.C., Notz, D., 2018. Changing state of Arctic Sea ice across all seasons. Environ. Res. Lett. https://doi.org/10.1088/1748-9326/aade56.

Sun, D., Held, I.M., 1996. A comparison of modeled and observed relationships between interannual variations of water vapor and temperature. J. Clim. 9, 665–675. https://doi.org/10.1175/1520 0442(1996)009<0665:ACOMAO>2.0.CO;2.

Taylor, K.E., Stouffer, R.J., Meehl, G.A., 2012. An overview of CMIP5 and the experiment design. Bull. Am. Meteorol. Soc. 93 (4), 485–498. https://doi.org/10.1175/bams-d-11-00094.1.

Tian, B., Fetzer, E.J., Kahn, B.H., Teixeira, J., Manning, E., Hearty, T., 2013. Evaluating CMIP5 models using AIRS tropospheric air temperature and specific humidity climatology. J. Geophys. Res.-Atmos. 118 (1), 114–134. https://doi.org/10.1029/2012jd018607.

Vihma, T., 2014. Effects of Arctic Sea Ice decline on weather and climate: a review. Surv. Geophys. 35, 1175–1214. https://doi.org/10.1007/s10712-014-9284-0.

Virts, Katrina S., Wallace, John M., Hutchins, Michael L., Holzworth, Robert H., 2013. Highlights of a New Ground-based, hourly global lightning climatology. Bull. Am. Meteorol. Soc. 94 (9), 1381–1391. https://doi.org/10.1175/bams-d-12-00082.1.